MODELING, IDENTIFICATION AND A FIRST CONTROL APPROACH ON THE QUALITY OF FLAMES IN OIL FURNACES

Agenor T. Fleury[a,b], Danilo S. Chui[b], Flavio C. Trigo[b], Flavius P. R. Martins[b]

[a] Centro Universitário da FEI, São Bernardo do Campo, SP, Brazil
[b] Escola Politecnica da Universidade de São Paulo, SP, Brazil

[a] agfleury@fei.edu.br, [b] danilochui@usp.br, [b] trigo.flavio@usp.br, [b] martins.flavius@usp.br

ABSTRACT
In industrial oil furnaces, unstable flames can lead to potentially dangerous conditions. Elaborate control systems are used to monitor the parameters of the process to avoid those problems. Current trends in research seek to identify *a priori* anomalous behavior of the flames, thus improving the time response of the control system. Controller performance is directly affected by the accuracy of the system model. Unfortunately, due to the complexity of the process, physical models of flame propagation are still not faithful enough for control purposes. Conversely, could the complex dynamics of flame propagation be described in terms of an identified assumed model, the control strategy could be improved. In this work, a control technique based on an Operational Modal Analysis model identification of a state-space description of oil flame dynamics in a prototype furnace is designed. Results obtained suggest that the proposed approach might be used in an automated control system.

Keywords: Flame modelling, Operational Modal Analysis, LQ control systems.

1. INTRODUCTION

The monitoring of oil-flame conditions in industrial petrochemical plants is of capital importance in terms of economy, environment-friendly operation, and safety. Currently, a wide array of sensors performs the task of measuring and informing the plant staff who, ultimately, judges the necessity of intervening to alter control parameters. This process has two drawbacks: firstly, sensors like thermocouples, flow meters, opacity meters, pressure sensor or even air-fuel ratio gauges are normally expensive and require frequent maintenance interventions; secondly, the judging ability of distinct operators is not the same, which might lead to below-standard functioning condition, including potentially dangerous ones. The first drawback pointed above should be tackled by replacing the specialized sensors by a frame-grabber and a set of low-cost CCD video cameras properly inserted in the furnace; those cameras can produce a continuous flow of flame images exhibiting luminance patterns that are well correlated to the physical combustion variables. The second drawback can be handled with computer vision routines able to identify normal or abnormal combustion states through the analysis of the sequence of flame images grabbed by the cameras. However, such an aim can not be successfully achieved unless the decision-making be supported by reliable inferences on the image processed data. That is why the computer vision based systems for combustion processes monitoring usually apply a heterogeneous set of statistical and artificial intelligence techniques, especially multivariate statistics, artificial neural networks and fuzzy logics.

Expert systems with these attributes are getting more and more importance for the oil and gas industries in the last years because of the potential impact to clean combustion. A key feature that must be monitored in order to maintain optimal burning conditions of oil flames is the vapor to fuel rate (VFR), which directly affects fuel nebulization and flame quality. Fleury *et al.* (2013) proposed a method based on computer vision and Kalman filtering to monitor nebulization quality of oil flames in a prototype refinery furnace. In short, the authors show that CCD-grabbed images of the flames at a priori known nebulization quality can be used to devise characteristic vectors that generate a set of fuzzy classification rules. Then, the components of a characteristic vector obtained from grabbed images of unknown a priori nebulization quality are assumed to be state-variables of a random-walk state-space model which, through a Kalman filter, effectively estimates the state and the nebulization quality when there is a statistically-proven convergence to a state that matches one of the classification rules. The researchers also state that the method could be improved once, instead of a random-walk model for the evolution of the state, a more accurate description of the system dynamics was employed. The difficulty that arises concerns the fact that phenomenological models available in the literature are poorly capable of encompassing both micro and macro scales occurring in flame propagation. As a consequence, a description based on either one would not cover the wide range of phenomena in between limiting conditions, thus resulting in a poor model under the estimation perspective.

Another important issue for the adequate operation of refinery furnaces is the early detection of flame instability. This phenomenon may cause the extinction of

the flame, resulting in an undesirable dangerous condition. Models for combustion instability in the literature (Bouziani *et al.*, 2005) based on coupled van der Pol equations state that unstable conditions can be detected under certain controlled situations; however, perturbations may induce false instability diagnosis near theoretically stable operation setups. Therefore, a description of the dynamics of the system based purely on data from observations of flames under actual operating conditions could possibly enhance the predictability of AI algorithms in general. A technique that suits this purpose is Operational Modal Analysis (OMA) in the time domain and, in a second paper (Silva *et al.*, 2015), authors proposed a new approach to estimate flame dynamics using OMA.

Overall, OMA seeks to identify parameters of an assumed model of the system dynamics using information from measurements of the system response to known particular inputs, namely, either step or impulse excitations, in real operating environment. The so called Ibrahim Time-Domain Method (ITDM), one of the tools available to perform the task, is widely employed in the identification of frequencies and modes of vibration in structures like stayed bridges (Liu *et al.*, 2012; Wu *et al.*, 2012), offshore platforms (Wang *et al.*, 2010), and components of rotating mechanisms (Grange *et al.*, 2009), just to cite some of the most recent publications.

An unconventional application of the ITDM was presented by Moura *et al.* (2010). Those researchers employed the technique to identify the discrete state transition matrix in electrical impedance tomography, one of the instances for which analytical models do not suffice to describe the evolution of the state, the resistivity distribution in a domain of interest, with the required accuracy. This suggests the power of the ITDM, in the sense of surpassing its original scope, once the modal decomposition approach enables avoiding complex (and, sometimes, quite inaccurate) modeling, even of highly non-linear systems.

Considering the previous discussion and the importance of combustion condition monitoring, this work proposes an extension of the paper by the same authors (Silva *et al.*, 2015) which addresses the problem of detecting evidence of the beginning of flame unstable behavior and automatically act to avoid such condition. The state transition matrix from a four-degree of freedom second order model of this phenomenon in a prototype furnace was already identified and a Linear Quadratic controller (LQ) is designed based on this dynamic model. This is a quite usual control approach, as should be done, for example, for the control of a flexible structure, except for the fact that the control system has to sustain flames in a nonzero condition, since this would imply flame extinguishment.

In the next sections, data collection and processing, a brief description of the ITDM, the LQ design and the first control results, with emphasis on the current approach are presented.

2. METHODS

Since modeling is a crucial requirement for a good control design, this section brings a discussion on the most important parts of author's previous work (Silva *et al.*, 2015). First aspect, experimental data were taken on a small-scale refinery furnace. Image data acquisition equipment is the same as mentioned by Fleury *et al.* (2013). The CCD camera for image grabbing is placed in a shielded and cooled compartment in the central cross-section of the furnace cylindrical wall. Burner inlets of primary and dry air, steam and oil enable the control of combustion parameters.

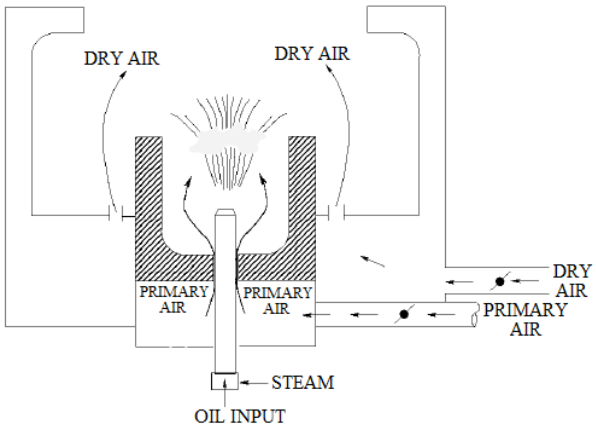

Figure 1: Burner Nozzle Schematics (modified from Fleury *et al.* (2013))

In order to correlate the visual appearance of the flames with the stability of the combustion process, three series of operational tests were carried out. Typical stability states, ranked according to a specialist, were obtained through proper regulation of the primary/secondary air rate (PSAR) at the burner nozzle, as depicted in the detail of Figure 1. Those series, encompassing an amount of 280 images, will be nominated hereafter as 'stable flames (PSAR=1.0)', 'unsteady flames (PSAR=1.86)' and 'unstable flames (PSAR=4.0)'. As illustrated by Figure 2 (a)-(b)-(c), the visual appearance of those image flames are clearly distinct, since the spatial distribution and arrangement of their pixel gray levels give rise to different types of texture.

The previous assertion was taken into account to construct a discriminant characteristic vector $\overrightarrow{v_i}$ based on 13 properties directly related to the texture and spatial distribution of the pixel gray levels of the flame image I_i. The components of $\overrightarrow{v_i}$ correspond to the following image properties:

(a)

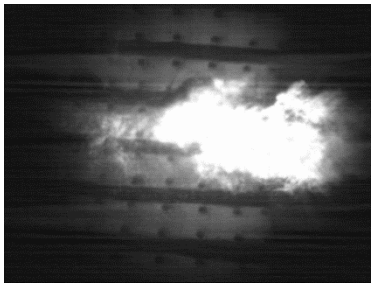

ISBN 978-88-97999-63-8; Bruzzone, Dauphin-Tanguy, Junco and Longo Eds.

(b)

(c)

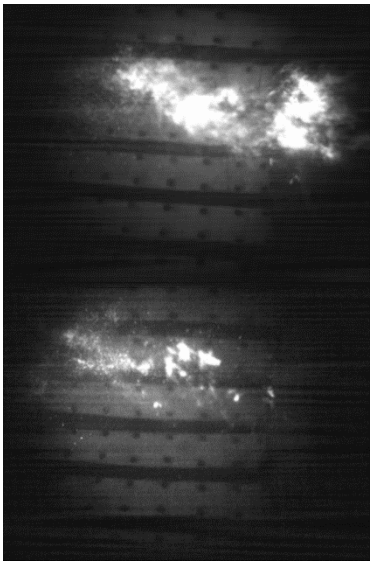

Figure 2: Flame Images. (a) PSAR=1.0; (b) PSAR=1.86; (c) PSAR=4.0.

- $v_i[1]$ is the average pixel gray level;
- $v_i[2]$ is the image entropy: $v_i[2] = -\sum_{j=1}^{N} p_j \log_2(p_j)$, where p_j is the frequency occurrence of gray level j;
- $v_i[3]$ is the average local maximum pixel gray level difference observed through a complete image scanning by a 3x3 window;
- $v_i[4]$ is the average local maximum mean standard deviation observed through a complete image scanning by a 3x3 window;
- $v_i[5]$ to $v_i[13]$ are texture characteristics based on the co-occurrence matrix (Gonzalez and Woods, 1992) of the image I_i, relative to two horizontally neighbor pixels whose gray levels are separated by either 1, 3 or 5 units. This way, $v_i[5]$, $v_i[6]$, and $v_i[7]$ are the correlation indexes of the number of occurrences of sequences of two pixels i and j whose gray levels are separated by 1, 3 and 5 units, respectively. Those indexes are calculated according to:

$$\sum_{i,j} \frac{(i-\mu i)(j-\mu j)\,p(i,j)}{\sigma_i \sigma_j} \qquad (1)$$

where $p(i,j)$ is the frequency occurrence of two horizontally pixels exhibiting gray levels i and j, μ_i and μ_j are the average number of occurrences of gray level pixels i and j, and σ_i, σ_j are their corresponding mean standard deviation. Similarly, $v_i[8]$, $v_i[9]$, and $v_i[10]$ are the contrast values of the number of occurrences of sequences of two pixels i and j whose gray levels are separated by 1, 3 and 5 units, respectively. Those indexes are calculated according to:

$$\sum_{i,j} |i-j|^2 \, p(i,j) \qquad (2)$$

Finally, $v_i[11]$, $v_i[12]$, and $v_i[13]$ are the homogeneity values of the number of occurrences of sequences of two pixels i and j whose gray levels are separated by 1, 3 and 5 units, respectively. Those measures are calculated according to:

$$\sum_{i,j} \frac{p(i,j)}{1+|i-j|} \qquad (3)$$

3. IBRAHIM TIME-DOMAIN METHOD

The ITDM was conceived in the 1970s and has, since then, been developed and successfully applied. The methodology here presented is a concise version of a work by Pappa and Ibrahim (1981), which reviews a series or previous research since Ibrahim and Mikulcik (1973).

Essentially, as originally devised, the method infers modal properties of a *n*-degree of freedom 2nd order assumed model from the free-response of a system to either impulsive or other excitation function (Ewins, 2000). By hypothesis, the dynamics of the system is represented by the equation:

$$M\,\ddot{y} + C\,\dot{y} + Ky = f \qquad (4)$$

in which M is the mass matrix, C is the damping matrix and K is the stiffness matrix, y, $\dot{y}$, $\ddot{y}$ respectively represent displacement, velocity and acceleration vector, while f stands for the exogenous forcing vector. Once this model is mapped into a state-space framework and the resulting $2n$ first order differential equations are written in matrix form, a so called $2n \times 2n$ system matrix conveys all information concerning inertia, stiffness and damping characteristics of the system under analysis.

As it is known from dynamic system theory, the *eigenvalues* of the system matrix are used to compute natural frequencies and damping factors, whereas its *eigenvectors* provide mode shapes, for each degree-of-freedom of the assumed model. Thus, provided that the system undergoes free vibration, Ibrahim's method estimates the above-mentioned matrix. Thus, naming x the state vector and A the system matrix, for a certain instant t_i, a set of displacements, velocities and acceleration measurements of the free-response of the system yield n linear equations to solve for $2n^2$ unknowns according to Eq. (5),

$$\dot{x}_j = Ax_j \qquad (5)$$

When measurements for $2n$ instants t_1, t_2, …, t_{2n}, are made, then one comes up with $2n^2$ equations, as follows:

$$[\dot{x}_1 \;\; \dot{x}_2 \ldots \dot{x}_{2n}] = A[x_1 \;\; x_2 \ldots x_{2n}] \qquad (6)$$

$$\dot{X} = AX \rightarrow A = \dot{X}X^{-1} \qquad (7)$$

Hence, considering that all the components of X and dX/dt are available, matrix A is unambiguously obtained, as it can be realized from Eq. (7). Regarding that the characteristic equation for the free-response of the system in Eq. (4) is:

$$\lambda^2 M + \lambda C + K = 0 \tag{8}$$

the solution of Eq. (7), at any measuring spot j, may be written as the sum of the contribution of each individual mode at that spot; for a given instant t_j,

$$x_j(t_i) = \sum_{k=1}^{2n} \psi_{jk} e^{\lambda_k t_i} \tag{9}$$

in which ψ_{jk} represents the free-response of the mode associated to the k[th] eigenvector at the j[th] spot, and λ_k the corresponding eigenvalue, solution of the characteristic equation, in general, both complex numbers. When $2n$ points are measured at several time instants, after some algebraic manipulation, Pappa and Ibrahim (1981) prove that the sought system matrix A is part of an eigenvalue problem. It follows that the eigenvalues of matrix A, complex numbers of the form $\lambda_k = \beta_k + i\gamma_k$, and the roots of the characteristic equation, the eigenvalues of the spatial model of Eq. (1) (Ewins, 2000) $s_k = \sigma_k + i\omega_{d,k}$, are related by

$$\beta_k + i\gamma_k = e^{\{\sigma_k + i\omega_{d,k}\}\Delta t_1} \tag{10}$$

In the above equation, Δt_1 represents an arbitrary time-shift and, in view of Eq. (9), the scalars β_k and γ_k can be used to obtain the damped natural frequency, natural frequency and damping factor for each mode according to Eqs. (11)-(14) which, once associated to the eigenvectors, completely characterize the system dynamics.

$$\omega_{d,k} = \tan^{-1}\left(\frac{\gamma_k/\beta_k}{\Delta t_1}\right) \tag{11}$$

$$\zeta_k = \frac{\sigma_k}{\left(\sigma_k^2 + \omega_{d,k}^2\right)^{1/2}} \tag{12}$$

$$\omega_{n,k} = \frac{\omega_{d,k}}{\left(1 - \zeta_k^2\right)^{1/2}} \tag{13}$$

$$\sigma_k = \frac{1}{2\Delta t_1}\ln(\beta_k^2 + \gamma_k^2) \tag{14}$$

An important issue that avoids straightly employing either the original or the modified ITDM is the demand of data from the free-response of the system under evaluation. This problem arises in several field situations, for instance, the identification of large structures like buildings and bridges, whose free-response is virtually impossible to obtain since, at least, random excitation coming from the environment (wind, ground vibration transmitted to the structure *via* mechanical constraints) is always present. In the case of the present scope, a free-response would imply extinguishing the flame, a potentially dangerous operational condition. This difficulty can be surmounted when the ITDM is employed in conjunction with the Random Decrement Technique (Cole, 1971), also known as RANDOMDEC, since demonstrated by Ibrahim and Mikulcik (1977).

The RANDOMDEC technique uses data from random excitation to estimate the free-response of the system. Cole (1971) asserts that, for a system vibrating under random stationary excitation, when the average of numerous samples of the displacements response are computed, the contribution of velocities and accelerations on the measured signal gradually vanish; consequently, the free-response is obtained. The *RANDOMDEC signature* of the system, as named by Cole, is computed using segments of the measured displacement signal delimited by the same boundary condition (a chosen amplitude, for instance). First, N equal time-length τ segments of the measured signal $y(t)$, starting at instants t_j (j=1, 2...N) provided that $y(t_j) = \alpha$ (the boundary condition) are sampled. Subsequently, the signature is obtained according to Eq. (15), the sought free-response of the system.

$$\delta(\tau) = \frac{1}{N}\sum_{j=1}^{N} y(t_j + \tau) \tag{15}$$

In this work, the RANDOMDEC signature is computed from averages of segments with initial value (boundary condition) ranging from 60 to 80% of the maximum amplitude. A four degree-of-freedom second order system model with viscous damping was admitted for the application of the ITDM. Owing to the availability of only one measuring station (the housing for the camera in the furnace wall), the procedure outlined by Pappa and Ibrahim (1981) was employed to fill the response matrix and the time-shifted response matrix, in the following way: lines at the upper half of the response matrix received data collected at lagging intervals of 1/24 and 1/8 seconds; data on the upper four lines, further delayed in 7/24 seconds, completed the lower four lines. The lagged response matrix, on the other hand, was obtained through a time-shift of 5/6 seconds of the elements of the response matrix. Finally, 12 time-instants were used by the ITDM.

4. MODELING RESULTS AND DISCUSSION

Grabbed images from the unstable flame condition (PSAR=4.0) were processed according to the description of Section 2, providing a set of vectors $v_i(t_k),\ i = 1,\ldots,13,\ k = 1,\ldots,100$, corresponding to a temporal sequence from available data of short-period trials for each of the 13 image characteristics. This reduced number of results poses another difficulty to the utilization of the RANDOMDEC technique: according to

Cole (1971), the procedure is as accurate as the number of averages in Eq. (12) increases. One manner to deal with this problem is by vectorizing v_i so as to obtain a longer sequence and improve algorithm performance, an artifice whose justification is based on the rationale that follows.

In the first place, the stationarity hypothesis was admitted as a requirement to the RANDOMDEC scheme, which implies that grabbed data (images) represents a stochastic process. The instantaneous components of each of the characteristic vectors v_i are obtained from the same data sample through strictly deterministic algorithms; furthermore, this sample contains information concerning the whole process at that instant. Therefore, it is fair to admit that the process is also wide-sense ergodic. As a consequence, the proposed vectorization will preserve the two first moments of the entire process. Offset cancellation and normalization of each sequence of parameters were performed before the vectorization process, whose outcome for the PSAR=4,0 is featured in Figure 3. The 'relative amplitude' instead of physical units at the ordinates label is thereof justified. The RANDOMDEC/ITDM was, then, employed to compute the modal parameters of the model, which can be seen in the second and third columns of Table 1.

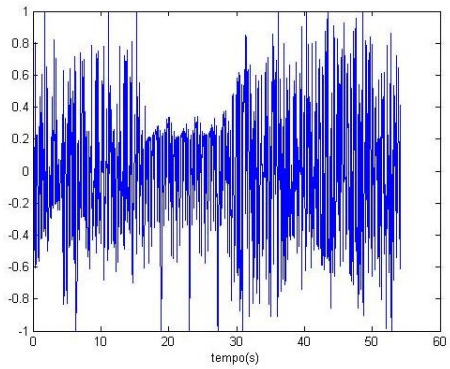

Figure 3: Vectorized Time-History of Characteristic Parameters for the 'Unstable' Flames ($PSAR = 4.0$)

In order to corroborate the above results, a spectral analysis of the temporal sequence of Figure 3 was performed and provided the power spectrum depicted in Figure 4, on which is possible to realize the spreading of the signal power throughout the whole range of identifiable frequencies, namely, from 0 to 12 Hz, including peaks at the four frequencies obtained by the ITDM/RANDOMDEC technique. The occurrence of several spurious frequencies among those identified can be explained by leakage arising from the convolution with a rectangular window before the spectral analysis. Nevertheless, the four frequencies of interest do present higher relative amplitudes. For the sake of comparison, the third and fourth columns of Table 1 show, respectively, natural frequencies computed by Fast Fourier Transform (FFT) and their relative discrepancy to the ones obtained with by the proposed approach. Overall, the errors may be considered negligible except for the second natural mode.

Table 1: Damped Natural Frequencies/ Damping Factors for Each Identified mode and Discrepancy Among Frequencies Computed from ITDM/ RANDOMDEC and Spectral Analysis.

Natural mode	ITDM-Rd damped natural frequency $f(Hz)$/ damping factor ζ	FFT damped natural frequency $f(Hz)$	$\frac{f_{FFT} - f_{Rd/MI}}{f_{Rd/MI}} \times 100$
1	1.88/0.072	1.88	0.0
2	2.41/0.740	2.88	19.5
3	3.60/0.791	3.40	-5.5
4	5.03/0.005	5.07	-0.8

The next step concerns the validation of the proposed approach; to this end, it suffices to verify whether data from stable ($PSAR = 1.0$) and partially stable ($PSAR = 1.9$) flame conditions, once processed according to ITDM/RANDOMDEC technique with parameters tuned for the unstable condition, can be distinguished from the latter. A further ratification is possible by reversing the process, *i.e*, using the ITDM/RANDOMDEC to identify stable flames and check the parameters thus found against partially stable and unstable flames. The results of both analyses are described below.

Spectra of signals reconstructed from the identified models, normalized by each relative amplitude, are depicted in Figure 4(a) and Figure 4(b), whose reference spectra are respectively the curves for $PSAR = 4$ and $PSAR = 1.0$. According to common sense reasoning, one should expect closer resemblance between curves of PSARs 1.9 and 4.0 in Figure 4(a) whereas, in Figure 4(b), curves of PSARs 1.9 and 1.0 would presumably look more alike. This qualitative analysis, however, does not provide solid ground for a definitive validation of the method since, in the first case, a clear match occurs once, at the 3.41 Hz frequency; on the other hand, in the second case, frequency matches occur close to abscissae 1.3 and 5.7 Hz.

(a)

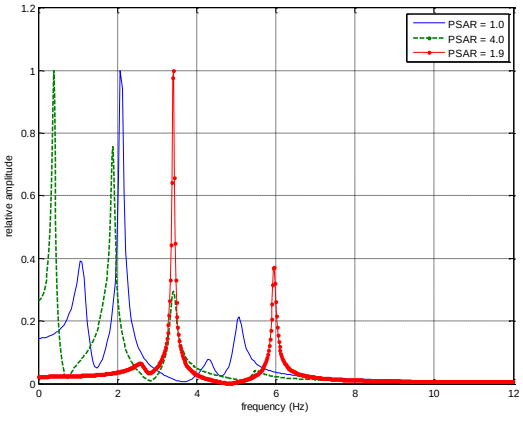

(b)

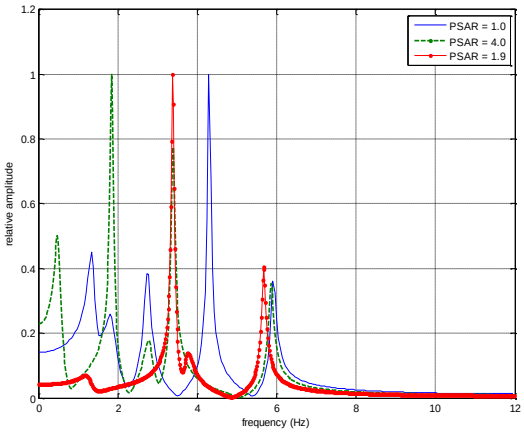

Figure 4: Comparative Relative Power Spectra for Identified Models of (a): Unstable ($PSAR = 4.0$); and (b): Stable ($PSAR = 1.0$) Reference Flames.

A quantitative measure of the adherence between an estimated mode and a reference mode which is normally used in OMA is the Modal Assurance Criterion - MAC (Ewins, 2000). The MAC essentially computes cumulative least-squares differences of all the combinations of pairs of data from distinct sets into a single scalar, despite that mode shapes and frequencies may be complex-valued. In the present case, the MAC has been modified to provide separate summations of the squared differences among frequencies and amplitudes of the reference and the other spectra in both cases under consideration.

Upon naming Nr: number of reference signals; Nt: number of test signals; Nrp: number of peaks of the reference signals; Ntp: number of peaks of the test signals; t: superscript related to test; r: superscript related to reference; F computation index related to frequency; and A: computation index related to amplitude, the criterion can be mathematically stated according to:

$$(MAC_F)_{Nr} = \sum_{i=1}^{Nt}\sum_{j=1}^{Nrp}\sum_{k=1}^{Ntp}\left(F_{j,k}^{t} - F_{j,k}^{r}\right)_i^2, \quad Nr = 1,2 \tag{16}$$

$$(MAC_A)_{Nr} = \sum_{i=1}^{Nt}\sum_{j=1}^{Nrp}\sum_{k=1}^{Ntp}\left(A_{j,k}^{t} - A_{j,k}^{r}\right)_i^2, \quad Nr = 1,2 \tag{17}$$

$$MAC = 1 - \frac{MAC_F \times MAC_A}{\max(MAC_F, MAC_A)} \tag{18}$$

Eq. (16) and Eq. (17) represent a quantitative measure of the scattering of frequencies and relative amplitudes around respective their references, whereas Eq. (18) expresses, in a single scalar, the combined effect of both dispersions. Thus, stable or partially stable flames, when tested using parameters computed from unstable flames, are expected to exhibit increasing values of MAC (partially stable > stable); conversely, unstable or partially stable flames should present decreasing values of MAC if probed against stable flames identified model. The results of the above validation are presented in Table 2, from which it is possible to confirm the truthfulness of those hypotheses.

Table 2: MAC Values for Cross-Validation of the Qualitative Analysis.

MAC		test PSAR		
		1.0	1.9	4.0
reference PSAR	4.0	0.0	0.67	1
	1.0	1.0	0.75	0.0

The validation step ends the whole proposed process for detecting evidence of the beginning of flame instability. Recalling what was mentioned in the introductory section, it is now possible to collect, from Eq. (10), the proper components of the discrete-time state transition matrix A, thus characterizing the dynamics of the system in the time domain, as it was initially proposed. Moreover, time-history of characteristic vector can be reconstructed from the identified system model and, as a consequence, one is able to infer how long flames with those features would take to be extinguished. The time-evolution of both measured and reconstructed characteristic vectors is shown in Figure 5, from which it can be asserted that unstable flames would last less than 20 seconds before total extinction.

It is important to point out that, in comparison to the previous work of Fleury *et al.* (2013), in which the white Gaussian noise represented the dynamics of flame propagation (in a state-space random walk model), the current research has been able to identify a second-order four degree-of-freedom model that describes the time evolution of the combustion process. Furthermore, data compression resulting from the application of modal identification, a feature that was not present in the previous work, tends to enhance the discrimination ability of the system, since redundancy is diminished.

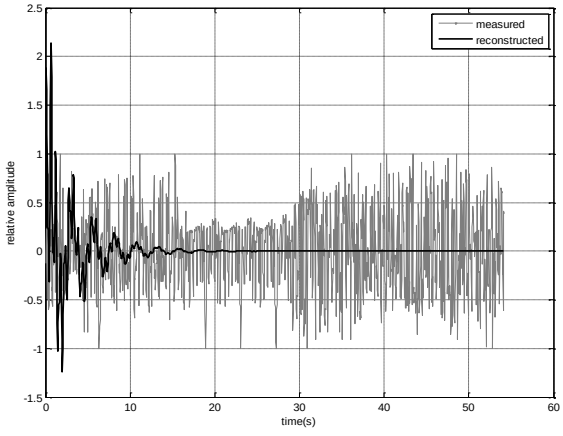

Figure 5: Comparative time-evolution of measured and reconstructed characteristic vectors for flames with PSAR = 4.0.

5. A CONTROL APPROACH

The identified four modes from ITDM/RANDOMDEC give rise to an experimental model. Here, frequencies and damping factors used in the experimental model are those described in Table 3.

Table 3: Identified Modes (Silva *et al.*, 2015).

Natural mode	Damped natural frequency f (Hz)	Damping factor ζ	Natural frequency ω_n (rad/s)
1	1.88	0.072	11.84
2	2.41	0.740	22.51
3	3.60	0.791	36.97
4	5.03	0.005	31.60

Thus, each mode can be represented as a second order system. Together, all four modes derive into an eighth degree dynamic system of the form:

$$\begin{matrix} \dot{\mathbf{x}} = \mathbf{A}\mathbf{x} + \mathbf{B}\mathbf{u} \\ \mathbf{y} = \mathbf{C}\mathbf{x} \end{matrix}, \qquad (19)$$

where $\mathbf{x} = [x_1 \quad \dots \quad x_8]^T$, $\mathbf{u} = [u_1 \quad \dots \quad u_4]^T$, $\mathbf{y} = [y_1 \quad \dots \quad y_8]^T$ and:

$\mathbf{A} = \mathbf{diag}[\mathbf{A_i}]$, $\mathbf{A_i} = \begin{bmatrix} 0 & 1 \\ -\omega_{ni} & -2\zeta_i\omega_{ni} \end{bmatrix}$, $i = 1, \dots, 4$

$\mathbf{B} = \mathbf{diag}[\mathbf{B_i}]$, $\mathbf{B_i} = \begin{bmatrix} 0 \\ 1 \end{bmatrix}$, $i = 1, \dots, 4$

For the sake of simplicity, let us consider that the output vector **y** and the state vector **x** have the same dimension. Of course, for other cases, one could design an observer to obtain the whole state. Thus, $\mathbf{C} = \mathbf{I_{8x8}}$.

System (19) characterized above describes the dynamics of the flame, in respect of the modes derived from the images from the CCD camera. Each subsystem is a classic underdamped second order system, whose responses fade to zero in the absence of a permanent input signal. Recurring to the system of the flame, the absence of oscillation means that the flame had extinguished. Therefore, one way to maintain the flame is to excite it with an appropriate input so that all four modes never stabilize asymptotically to a position. The strategy is to maintain the system into an oscillatory movement, therefore assuring the flame characteristics for the time needed. This behavior can be obtained if an appropriate reference is defined and a simple LQR control is synthetized to follow this reference.

5.1. Reference definition

Reference will be defined in accordance to the desired behavior for system (19). A slight modification on system (19) would be enough to give it an oscillatory characteristic. Let us mirror the system (19) but modify matrix **A** setting all damping factors $\zeta_i = 0$. That would make the subsystems to behave like undamped second order systems. Thus, consider the following reference system:

$$\dot{\mathbf{x}}_\mathbf{r} = \mathbf{A_r}\mathbf{x_r} + \mathbf{B_r}\mathbf{u_r} \qquad (20)$$

where $\mathbf{x_r} = [x_{r1} \quad \dots \quad x_{r8}]^T$, $\mathbf{u_r} = [u_{r1} \quad \dots \quad u_{r4}]^T$, $\mathbf{B_r} = \mathbf{B}$ and:

$\mathbf{A_r} = \mathbf{diag}[\mathbf{A_{ri}}]$, $\mathbf{A_{ri}} = \begin{bmatrix} 0 & 1 \\ -\omega_{ni} & 0 \end{bmatrix}$, for $i = 1, \dots, 4$

In order to define completely the reference path, it is necessary to set up an initial condition for the reference system, $\mathbf{x_0} = [0.5 \quad 0 \quad 0.5 \quad 0 \quad 0.5 \quad 0 \quad 0.5 \quad 0]^T$ and define the input, for all time $t \geq 0$, $\mathbf{u_r} = [0 \quad 0 \quad 0 \quad 0]^T$. These conditions could be interpreted, in an analogous mass-spring mechanical system, as an arbitrarily chosen initial position at $0.5\,m$, with initial velocity of the mass equal to zero, for each subsystem of (20). Moreover, the position of equilibrium of these mass-spring subsystems is also arbitrarily set to $1.0\,m$. As expected, the reference system responses are composed of a set of oscillatory movements shown in Figure 6 and Figure 7.

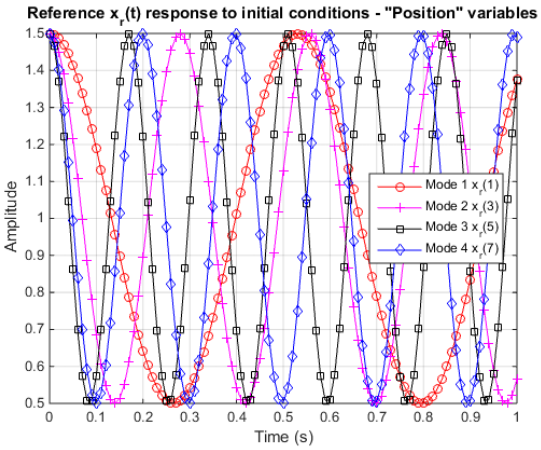

Figure 6: Reference $\mathbf{x_r(t)}$ Response to Initial Conditions for "Position" Variables

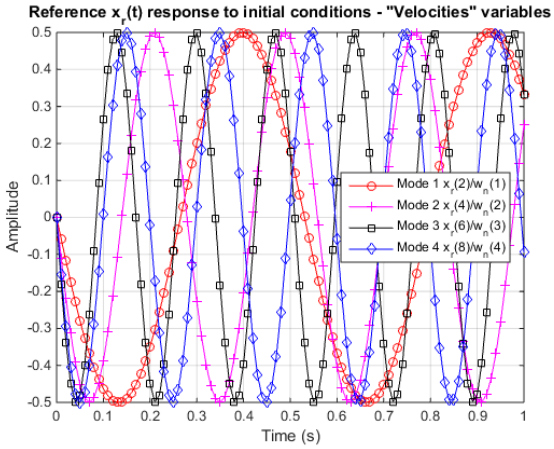

Figure 7: Reference $\mathbf{x_r(t)}$ Response to Initial Conditions for "Velocities" Variables

5.2. LQ Controller

Let us define the vector **e** the error of the system:

$$\mathbf{e} = \mathbf{x} - \mathbf{x_r} \qquad (21)$$

Then,

$$\begin{aligned} \dot{\mathbf{e}} &= \dot{\mathbf{x}} - \dot{\mathbf{x}}_\mathbf{r} = \mathbf{A}\mathbf{x} + \mathbf{B}\mathbf{u} - \mathbf{A_r}\mathbf{x_r} - \mathbf{B_r}\mathbf{u_r} \\ \dot{\mathbf{e}} &= \mathbf{A}(\mathbf{e} + \mathbf{x_r}) + \mathbf{B}\mathbf{u} - \mathbf{A_r}\mathbf{x_r} - \mathbf{B_r}\mathbf{u_r} \\ \dot{\mathbf{e}} &= \mathbf{A}\mathbf{e} + (\mathbf{A} - \mathbf{A_r})\mathbf{x_r} + \mathbf{B}\mathbf{u} - \mathbf{B_r}\mathbf{u_r} \end{aligned} \qquad (22)$$

Now, let us define the augmented state variable vector $\bar{\mathbf{x}} = [\mathbf{e} \quad \mathbf{x_r}]^T$ and the input vector $\bar{\mathbf{u}} = [\mathbf{u} \quad \mathbf{u_r}]^T$ that will have to satisfy the following dynamic system:

$$\begin{matrix} \dot{\bar{\mathbf{x}}} = \bar{\mathbf{A}}\bar{\mathbf{x}} + \bar{\mathbf{B}}\bar{\mathbf{u}} \\ \mathbf{y} = \bar{\mathbf{C}}\bar{\mathbf{x}} \end{matrix}, \tag{23}$$

where,

$$\bar{\mathbf{A}} = \begin{bmatrix} \mathbf{A} & \mathbf{A} - \mathbf{A_r} \\ \mathbf{0_{8x8}} & \mathbf{A_r} \end{bmatrix}, \bar{\mathbf{B}} = \begin{bmatrix} \mathbf{B} & -\mathbf{B_r} \\ \mathbf{0_{8x4}} & \mathbf{B_r} \end{bmatrix} \text{ and } \bar{\mathbf{C}} = \begin{bmatrix} \mathbf{C} & \mathbf{C_r} \end{bmatrix}$$

If the error $\mathbf{e(t)}$ goes to zero, it means that the system (19) is following the reference (20). To close the control loop and achieve zero error, a linear input $\bar{\mathbf{u}}(\mathbf{t})$ is defined for the system (23):

$$\begin{aligned} \bar{\mathbf{u}} = -\mathbf{K}\bar{\mathbf{x}} \Leftrightarrow \begin{bmatrix} \mathbf{u} \\ \mathbf{u_r} \end{bmatrix} &= \begin{bmatrix} -\mathbf{k}_e & -\mathbf{k_r} \\ -\mathbf{k_e^r} & -\mathbf{k_r^r} \end{bmatrix} \begin{bmatrix} \mathbf{e} \\ \mathbf{x_r} \end{bmatrix} \\ &= \begin{bmatrix} -\mathbf{ke} - \mathbf{k_r x_r} \\ -\mathbf{k_e^r e} - \mathbf{k_r^r x_r} \end{bmatrix} \end{aligned} \tag{24}$$

Gain matrix $\mathbf{K}$ is determined through the LQR controller method. This method minimizes the performance index J:

$$J = \int_0^\infty \bar{\mathbf{x}}(\mathbf{t})^T (\mathbf{Q} + \mathbf{K}^T \mathbf{R} \mathbf{K}) \bar{\mathbf{x}}(t)\, dt, \tag{25}$$

where $\mathbf{Q}$ is a positive semidefinite matrix and $\mathbf{R}$ is a positive definite matrix and are chosen as follows:

$$\begin{matrix} \mathbf{Q} = \begin{bmatrix} \mathbf{Q}' & \mathbf{0_{8x8}} \\ \mathbf{0_{8x8}} & \mathbf{0_{8x8}} \end{bmatrix}, \\ \mathbf{Q}' = \mathbf{I_{8x8}} \cdot [1 \;\; 30 \;\; 1 \;\; 10^4 \;\; 1 \;\; 2x10^4 \;\; 1 \;\; 10]^T \\ \mathbf{R} = \mathbf{I_{8x8}} \end{matrix} \tag{26}$$

One can find the gain matrix $\mathbf{K}$, through the solution algebraic of the Ricatti equation that results from (25).

5.3. Simulation results

Simulation was performed considering that a flame is ongoing and the control is suddenly turned on to maintain it. The vector of initial conditions was arbitrarily chosen from positive realizations of Gaussian distributions with mean 1 and 0 respectively for "position" and "velocity", and variance 1 for all state variables.

As it is observed from Figure 8 to Figure 11, the control action was able to make the system dynamics follow the desired reference within few seconds.

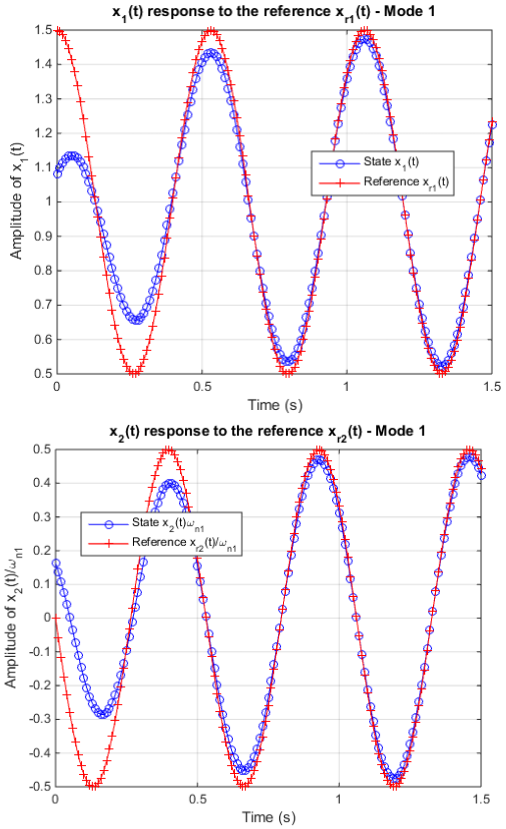

Figure 8: Mode 1 Response to Reference Tracking Control

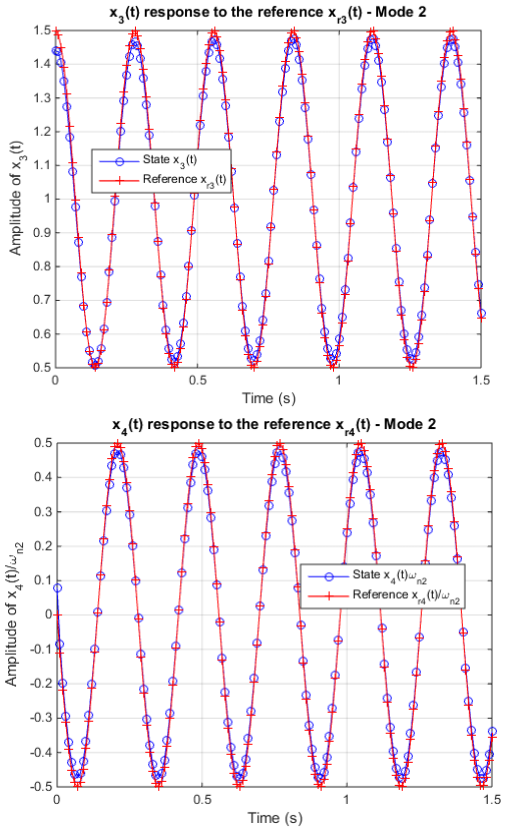

Figure 9: Mode 2 Response to Reference Tracking Control

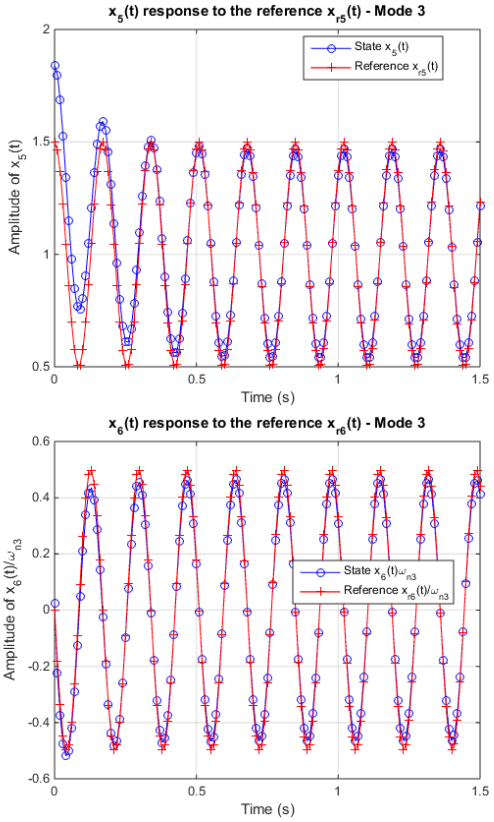

Figure 10: Mode 3 Response to Reference Tracking Control

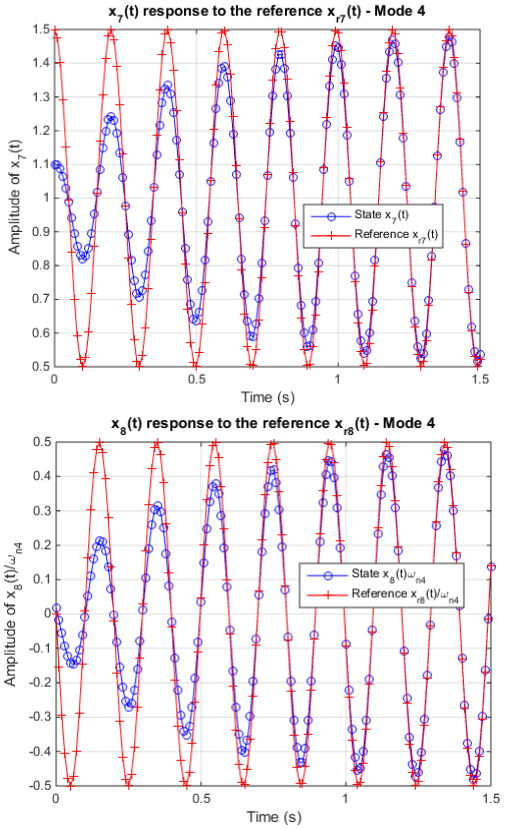

Figure 11: Mode 4 Response to Reference Tracking Control

6. CONCLUSIONS

This work has proposed a new approach to identify and control the dynamics of oil-flames in a prototype furnace. A time-domain method (ITDM) was employed in conjunction with the random decrement technique to identify an assumed four degree-of-freedom second order model of unstable flames from computer-vision processed grabbed images of CCD cameras. A Linear-Quadratic Controller was then designed based on the modal model identified for a *priori* known flame conditions, corroborated by qualitative and quantitative comparison with the outcomes of traditional spectral analysis of their reconstructed temporal signals.

The work must be considered a first incursion towards a complete control system able to assure clean combustion in oil furnaces. Achievement of a control system with attributes like this will require more sophisticated control techniques and, most important, an algorithm to correlate flame images to control actions. The choice for a cheap control technique (LQ) here is justified by the fact that the adaptive-predictive methods to be investigated are based on linear-quadratic approaches. The promising results achieved here using LQ design indicate a feasible way. Nevertheless, the topic control of oil furnaces is a fascinating one and authors intend to bring other subjects to discussion in future publications.

REFERENCES

Bouziani, F., Landau, I. D., Bitmead, R. R., Voda-Besançon, A. (2005). An analyticallytractable model for combustion instability. In Proceedings of the 44th IEEE conference on decision and control, and the European control conference 2005 (pp. 7398–7403). Seville, Spain.

Cole, H. A. (1971). Failure Detection of a Space Shuttle Wing Flutter by Random Decrement. NASA, TMX-62.041.

Ewins, D.J. Modal Testing: Theory, Practice and Application, 2nd ed. (2000). Hersfordshire, MSP.

Fleury, A.T., Trigo, F.C., Martins, F.P.R. (2013). A new approach based on computer vision and non-linear Kalman filtering to monitor the nebulization quality of oil flames. Expert Systems with Applications, vol. 40(12), 4760-4769.

Gonzalez, R.C., Woods, R.E. Digital Image Processing, 3rd ed. (1992). New York, Addison-Wesley.

Grange, P., Clair, D., Baillet, L., Fogli, M. (2009). Brake squeal analysis by coupling spectral linearization and modal identification methods. Mechanical Systems and Signal Processing, vol. 23(8), 2575-2589.

Ibrahim, S.R., Mikulcik, E.C. (1973). A time domain modal vibration test technique. The Shock and Vibration Bulletin, Vol.43, Part 4, 21-37.

Ibrahim, S.R., Mikulcik, E.C. (1977). A Method for the Direct Identification of Vibration Parameters from the Free Response. The Shock and Vibration Bulletin, Vol. 47, Part 4, 183-198.

Liu, T.Y., Chiang, W.L., Chen, C.W., Hsu, W.K., Lin, C.W., Chiou, D.J., Huang, P.C. (2012). Structural

system identification for vibration bridges using the Hilbert-Huang transform. Journal of Vibration and Control, vol. 18(13), p. 1939-1956.
Moura, F.S., Aya, J.C.C., Fleury, A.T., Amato, M.B.P., Lima, R.G. (2010). Dynamic Imaging in Electrical Impedance Tomography of the Human Chest With Online Transition Matrix Identification. IEEE Transactions on Biomedical Engineering, vol. 57(2), p. 422-431.
Pappa, R.S., Ibrahim, S.R. (1981). A Parametric Study of the Ibrahim Time Domain Modal Identification Algorithm. The Shock and Vibration Bulletin, Vol.51, Part 3, p. 43-72.
Silva, R.P., Fleury, A.T., Martins, F.R.P., Ponge-Ferreira, W.A.J., Trigo, F.C.(2015) Identification of the State-Space Dynamics of Oil Flames through Computer Vision and Modal Techniques. Expert Systems with Applications, v42, p. 2421-2428.
Wang, S.Q., Zhang, Y.T., Feng, Y.X. (2010). Comparative Study of Output-based Modal Identification Methods Using Measured Signals from an Offshore Platform. Proceedings of the ASME 29th International Conference on Ocean, Offshore and Arctic Engineering, vol. 2, 561-567.
Wu, W.H., Chen, C.C., Liau, J.A. (2012). A Multiple Random Decrement Method for Modal Parameter Identification of Stay Cables Based on Ambient Vibration Signals. Advances in Structural Engineering, vol. 15(6), p. 969-982.

AUTHORS BIOGRAPHY

Agenor de Toledo Fleury has a degree in mechanical engineering from ITA / Aeronautics Technological Institute (1973), a Master's degree (1978) and PhD in Mechanical Engineering from the University of São Paulo (1985). He is currently professor at FEI University and a part-time PhD professor at the Polytechnic School, University of Sao Paulo. He has led various projects with emphasis on Dynamics and Control Systems. His most recent projects address modeling and control of nonlinear systems, optimal control and estimation, in applications of Biomechanics, Robotics and Automotive Engineering.

Danilo de Santana Chui received the B. Eng. degree in mechanical engineering from University of São Paulo (USP), São Paulo, Brazil, in 2003, the M. Eng. degree in mechanical and control engineering from Tokyo Institute of Technology (TITech), Tokyo, Japan, in 2006 and is currently a PhD student at University of São Paulo. He is an Assistant Professor in the Department of Mechanical Engineering at Federal University of Amazonas (UFAM). His research interests include nonlinear control, stochastic control and control applications to combustion processes and vehicle technologies.

Flávio Celso Trigo was born in São Paulo, Brazil, in 1961. He graduated in Mechanical Engineering in 1985 and received a PhD in Mechanical Engineering at the Polytechnic College, USP in 2005. Since 2008, he works as a professor/researcher at the Department of Mechanical Engineering, USP, Brazil. His main research interests include real-time parameter estimation and system identification through nonlinear techniques, flame dynamics modeling and controlling, simulation of offshore riser behavior, and sensor fusion for inertial guidance.

Flavius Portella Ribas Martins was born in São Paulo, Brazil, in 1956. He received BE degree in Naval Engineering from USP, 1979, and MSc in Naval Engineering and PhD degrees in Mechanical Engineering also from USP, in 1981 and 1999, respectively. Since July 2008, he has been with the University of São Paulo, São Paulo Brazil, as Assistant Professor at the Mechanical Engineering Department. His current research interests include theoretical mechanics, computer vision, and artificial intelligence. Dr Martins is a Fellow of the American Society of Mechanical Engineers.